Visual study of the freezing process of a water droplet on a horizontal copper plate

Zhe Zhang[1] | Shengnan Lv[1] | Sunil Mehendale[2] | Lei Yan[1] | Hui Yuan[3] | JinJin Tian[1]

[1]Tianjin Key Laboratory of Refrigeration Technology, Tianjin University of Commerce, Tianjin, 300134, China

[2]Manufacturing and Mechanical Engineering Technology, Michigan Technological University, Houghton, 49931, USA

[3]Veck (Tianjin) Co. Ltd., Tianjin, 301700, China

Correspondence

Zhe Zhang , Tianjin Key Laboratory of Refrigeration Technology, Tianjin University of Commerce, Tianjin, China, 300134

Email: zhangzhe@tjcu.edu.cn

ABSTRACT

Freezing on cold surfaces can cause equipment damage. To prevent the increase of ice, it is necessary to understand the freezing process of water droplets on the cold surface. This study based on the droplet shape analyzer, the freezing process of droplets is studied visually. The effects of the substrate temperature, ambient relative humidity, and volume of droplets on the freezing process were analyzed. It is found that the influence of ambient relative humidity and substrate temperature on the supercooling time are related to the degree of supercooling. When the substrate temperature is lower than the critical supercooling degree, the effect of substrate temperature and the ambient relative humidity on the supercooling time is weakened. With the increase of volume, the supercooling time decreases first and then increases. In the phase transformation stage, there is a positive correlation between the change of phase transformation time and the influencing factors.

KEYWORDS: Supercooling time, Freezing time, Solid volume fraction, Critical supercooling degree, Critical volume

1 | INTRODUCTION

The freezing process of droplets has long been a question of great interest in many fields, such as machinery [1], food [2, 3]and refrigeration [4, 5]. The icing on the surface of heat exchangers and aircrafts will pose a serious threat to equipment. The freezing of small droplets is the foundation of ice formation on cold surfaces and is a complex process. It is highly interdisciplinary, involving heat transfer, hydrodynamics, thermodynamics, materials science, and other important areas of knowledge. Thus, it is important to understand the freezing process of droplets. The results will help researchers to understand the underlying physics and develop more effective anti-icing or de-icing methods .

In studies of the shape change of the droplet during freezing, Marín et al. [6, 7] found that when freezing was completed, the droplet would form a bulge. The bulge was universal, independent of the substrate material and temperature, and the angle was about 139 ± 0.8 °. The experimental results of Ismail et al. [8] showed that asymmetric droplets would also form a bulge after freezing. The only factor affecting the bulge angle was the ice-water density ratio. Schulte et al. [9] observed the phase transition process inside the droplet and it qualitatively agreed with the predictions the semi-analytical subscale model they developed. In the simulation of droplet freezing they conducted, Zhang et al. [10, 11] examined the supercooling effect and the volume expansion during the phase transformation. Their simulation provided results very close to the experimental data. Gaurav et al. [12] studied the heat transfer inside the droplet based on the heat conduction equation. They found that in the early stages of freezing, the temperature of droplets on a cold hydrophobic surface decreased gradually, while on a cold hydrophilic surface, the temperature drop was relatively stable. As the freezing progressed, the temperature reduction rate of droplets on both types of surfaces obviously increased. Zhang et al. [13] found that a certain degree of supercooling was required at the beginning of droplet freezing. The droplet volume and height increased during the freezing process. Truong et al. [14] simulated the morphological changes of the droplet freezing process with different bond numbers (Bo). The final freezing height decreased with the increase of the Bo number. Haruka

et al. [15] studied the freezing behavior of droplets on inclined superhydrophobic surfaces. They concluded that the higher the initial temperature of the droplet, the lower the surface tension of the droplet. Thus, the contact area between the droplet and the substrate was increased, and it was easier for the droplet to adhere to the surface.

Some researchers have studied the effect of surface properties on droplet freezing. One study by Ludmila et al. [16] examined the effect of solid cold surfaces with different wettability on the freezing process of droplets. It was found that the contact angle of the droplets on a superhydrophobic surface was larger, which significantly delayed the freezing of the droplets compared to a hydrophilic surface. Further studies in this direction by Huang et al. [17] confirmed the findings of Ludmila et al. [16]. However, they also found that in the subsequent stage of freezing, the frost crystal growth on the droplet surface would be correspondingly greater. Through the study of the frosting process on a silicon wafer with different surface structures, Yue et al. [18] found that the surface microstructure also affected the freezing process of droplets. In a follow-up study, Hao et al. [19] found that a reduction in the roughness of the cold surface delayed freezing and prolonged the freezing time of the droplets. Markus and others [20] found that the frosting stage of a cold surface was related to the freezing stage of droplets. Adopting differential scanning calorimetry (DSC), Fang et al. [21] found that the solidification temperature of droplets on a high roughness and poor wettability surface was lower. Kuok et al. [22] discovered that an increase of surface wettability will accompany increased surface roughness, which will decrease the contact angle lag of droplets.

Some scholars have considered the influence of environmental factors on the freezing of droplets. For example, Gao Penghui et al. [23] put together a freezing model of droplets under the action of ultrasound. It was inferred that ultrasonic waves could increase the air bubble content, which enhanced the heat transfer and sped up the freezing of droplets. For the same ultrasonic wave intensity, the lower the frequency of the ultrasonic wave, the faster the droplet was seen to freeze. Dmitrii et al. [24] found through experiments and simulations that an electric

field could also affect the freezing of droplets. The higher the electric field intensity, the faster was the freezing rate. Faryar et al. [25] found that ambient relative humidity could affect the supercooling time of a droplet, which was related to the presence of tiny droplets around it. At lower ambient pressure, Jin et al. [26] found that evaporation occurs on the droplet surface, which then absorbed heat from the droplet and resulted in the droplet freezing faster.

Some researchers have also studied the freezing process of non-stationary droplets. Sultana et al. [27] found that if the flow of ambient air was enhanced, the heat exchange between the droplets and the environment would be enhanced, and the frost nucleation would be accelerated. Bin et al. [28] studied the effect of supercooling (TS) on freezing in the process of a droplet impinging on a sloping substrate. When TS was lower than -37.5 °C, the droplet did not rebound and the freezing time was shortened. Yao et al. [29, 30] experimentally and analytically studied the freezing process of a droplet when it impacted a cold surface. The critical temperature for the drop not to rebounce and the critical Weber number for droplet breakup were found.

Despite the fact that many researchers have studied the freezing process of droplets, most of them are not in a closed environment and are greatly affected by the fluctuation of environmental factors, as summarized above. This is not conducive to study the effect of a single factor on droplet freezing. In this study, an integrated test-bed DSA100 (KRÜSS GmbH, Germany) was used, and the experimental part was placed in a closed cavity. Experiments can more accurately control the influencing factors and exclude the influence of irrelevant factors. At the same time, based on the experimental results, a correlation is proposed to predict the supercooling time and solid volume fraction. It provides a certain theoretical basis for future researchers to predict the freezing behavior of droplets.

2 | EXPERIMENTAL EQUIPMENT AND TEST CONDITIONS

### 2.1 | Experimental equipment

2.1.1 | Droplet shape analyzer

Figure 1 is the schematic diagram of the droplet shape analyzer (DSA100) system. It is composed of five parts: droplet generator, video recording system composed of a high-resolution camera and LED light source, TC40 temperature control system, HC10 humidity control system, and analysis system. The experimental part of the DSA100 system is situated in the semi-sealed enclosure (TC40). TC40 contains a semiconductor refrigeration module to control the substrate temperature (with an error of 1°C). The temperature value is set by the temperature controller. The circulating water in the thermostatic water bath is used to take away the heat of semiconductor to avoid the influence on the internal temperature field. The temperature chamber of TC40 is combined with the humidity chamber of HC10 to achieve the control of temperature and humidity. HC10 controls humidity by blowing wet air into the interior through a channel on the back of the TC40. The humidity value is set by the computer. The DSA100 system incorporates high precision temperature sensor (TP20), which enables real-time acquisition of the temperature of the substrate, the measurement accuracy is 0.1°C. The titration and temperature measurement equipment can be in a relatively sealed environment. Since no human contact is involved in the test process, the error caused by various environmental interferences is significantly reduced, and highprecision measurement of samples is realized. This instrument uses ADVANCE control software (KRÜSS GmbH, Germany) to observe and study the freezing process of droplets on the cold surface. ADVANCE can realize fully automatic measurement with the following capabilities: electronic focusing and zoom control, automatic parameter setting of optical components, rapid and accurate measurement of sample movement, and measurement of surface free energy in a few seconds. The minimum measured accuracy of the system can reach 20 pL, and it can titrate several droplets at the same time. The titration syringe used by DSA100 is SY20, which is a 500μL glass syringe. Droplet size and titration position can be controlled by ADVANCE, and the error is within 5%. For image acquisition, prism optics are utilized, in which angle and brightness can be adjusted. A cold light source IL10 is used for

lighting in the whole process to reduce the interference of reflection in the image and to ensure clarity of the image collection and recording for very small droplets. Since the freezing of a droplet typically lasts only tens of milliseconds, the high-resolution camera CF3217 was employed to capture the dynamic image. The highest resolution of CF3217 is 1000 f/s, which is sufficient to clearly record the experiment.
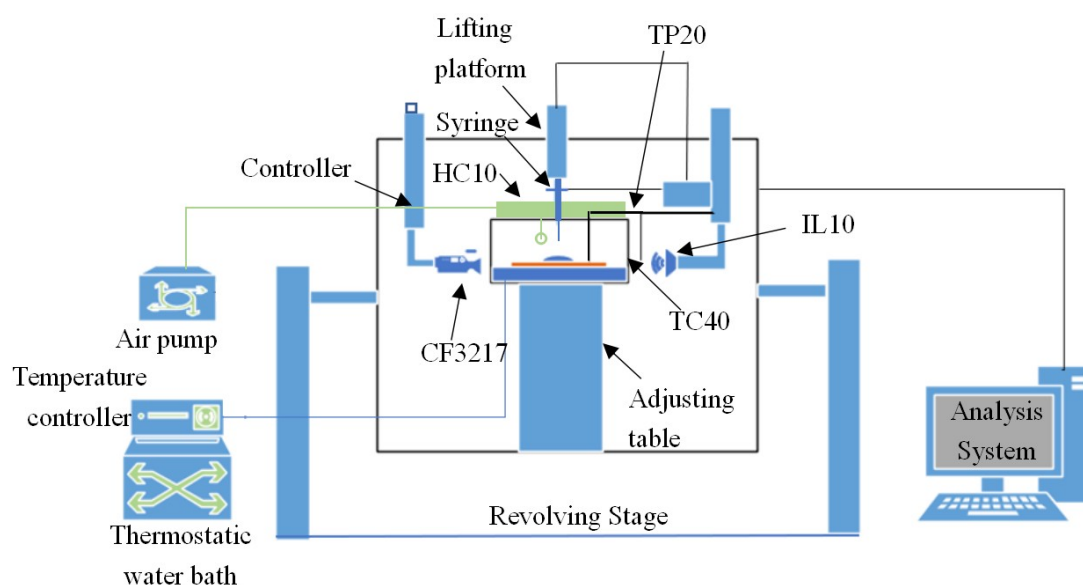

FIGURE 1 DSA100 system schematic diagram.

ADVANCE software basically provides a means of measuring angles. By setting the baseline position for the sample and selecting the best-fit method, the contact angle can be measured. The standard error was <5%. ADVANCE can carry out repeated measurements many times, which is convenient for data storage and comparison. In the current research, due to the roughness of the substrate, the droplets have small asymmetry. There will therefore be a slight difference between the left and right contact angles. To accurately express the contact angle of droplets, the left and right contact angles needed to be measured. To obtain accurate values of the contact angle, each contact angle is measured five times, and the average is taken to be the static contact angle of the surface. The contact angle measurement interface in ADVANCE is depicted in Figure 2.
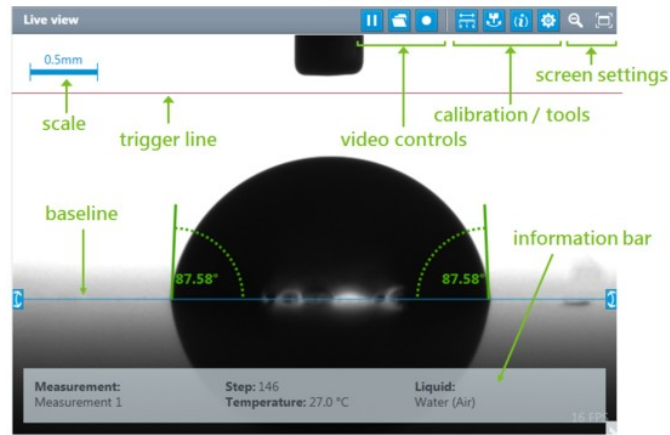
FIGURE 2 ADVANCE contact angle measurement interface.

## 2.1.2 | Three-dimensional surface topography measuring instrument

Figure 3 shows the three-dimensional surface topography measuring instrument (InfiniteFocus G5) device.

The instrument is a 3D optical measuring instrument with all-round and automatic functions. It can measure the

surface in all directions and is simple to operate with the help of a LED ring lamp. Vertical resolutions up to 10 nm

can be measured. The minimum measured roughness is 0.03μm.
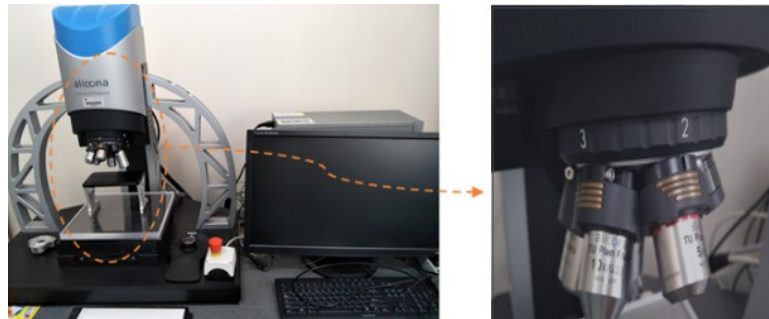
FIGURE 3 InfiniteFocus G5 device.

Before the experiment, the surface of copper was cleaned by an ultrasonic cleaner. This ensured proper initial

consistency of each experiment and reduced the experimental errors involved. After the cleaned copper plate was

naturally dried, it was placed in the InfiniteFocus G5 to measure the roughness. The size of the copper plate used

in the experiment was 80mm × 80mm × 0.02mm. It can be viewed in Figure 4 (a). Five points as shown in Figure

4 (a) were chosen to measure the roughness (R_a). Based on three measurements taken at each of the five points, the

average surface roughness was found to be R_a= 55.4 nm. The microstructure of the copper surface is presented in

Figure 4 (b).

(a)   (b)
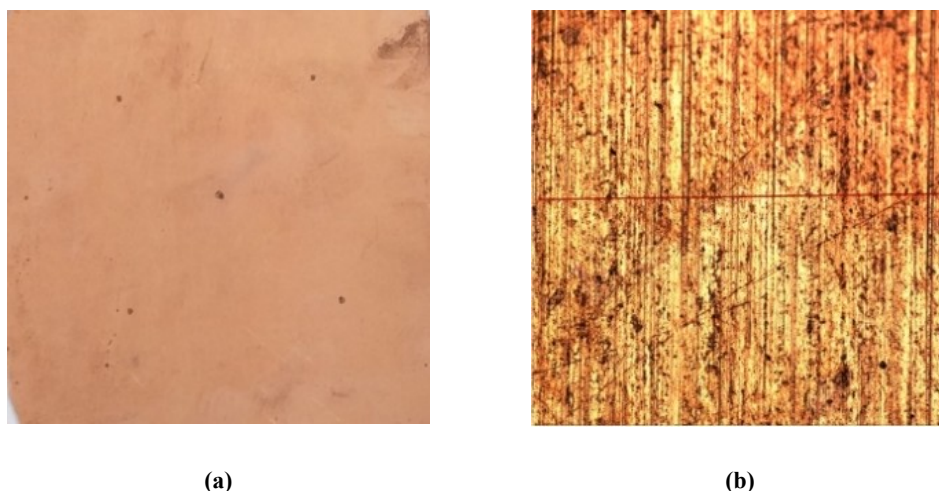
FIGURE 4 Schematic diagram of copper surface structure.

2.2 | Experimental method

First, all devices of the DSA system were powered on. Water circulation was then initiated to ensure that the

temperature controller and other equipment were functional after the the water was in circulation. To avoid the

influence of other conditions on the experiment, a cold light source was employed for illuminating the sample. The

following experimental information was entered in the ADVANCE software: titration method, sample test

interface, input test name, temperature, and test liquid information, etc. The height of the sample table was then

adjusted to align the sample surface with the baseline. With the image background color set to moderate

brightness, the Zoom knob was rotated to accommodate image size, and the camera was focused to obtain a clear

image.

After the equipment was adjusted as described above, SY20 was filled with deionized water and any

remaining air bubbles were discharged to ensure that the sample droplets were free from any trapped air. The

titration system (Doing & Syringe Function) was controlled by ADVANCE to produce the required volume of

droplets. The needle was then lowered to place the droplet on the sample surface such that the droplets could

appear clearly in the center of the viewing field, and then the needle was lifted. The refrigeration power supply was then turned on to cool down the copper plate to the set value. To get more intuitive results, the timing was started when the substrate temperature reached 0°C. The phase transformation moment was defined as time t=0s, and hence the supercooling time was negative. The recording software was used to take pictures of the freezing process of droplets. To reduce the random error involved, each experiment was repeated five times.

The whole experiment was carried out in the TC40 (-30°C ~ 160°C), maintaining stable values of temperature and humidity. The ambient temperature and the initial temperature of the droplets were 27.2 ± 0.5°C. Different substrate temperatures Tw (-7.5~-17.5°C), ambient relative humidity φ (32~62%), and droplet volume V (1~10 μL) were set for the experiments, and the parameter error was controlled within 1%. The dynamic process of droplet freezing was photographed for visual research. At the end of the experiment, the collected video was transmitted to the ADVANCE software on the computer for contact angle measurement. Morphological changes and freezing times were observed in the image sequence.

3 | EXPERIMENTAL RESULTS AND ANALYSIS

3.1 | The effect of substrate temperature
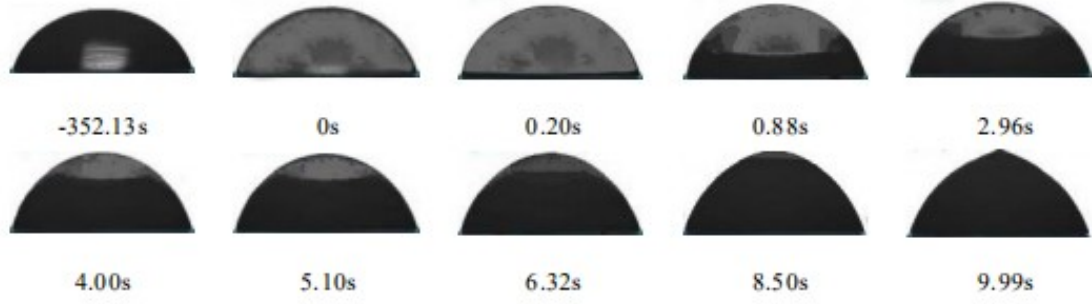
3.1.1 | Freezing process

According to previous studies, the freezing process of droplets can be divided into four stages: supercooling, rewarming, phase transformation, and cooling[31]. However, the duration of the rewarming stage is very short and the study of the cooling process is meaningless. Therefore, this study did not discuss the changes in droplets in these two stages.

Figure 5 presents the image sequences of 5 μL droplets undergoing freezing at four different substrate temperatures (-7.5°C, -10.5°C, -13.5°C, and -17.5°C). The ambient temperature was 27.2°C and the relative humidity was 62%. It can be seen from the figure that the freezing patterns of droplets were similar for the
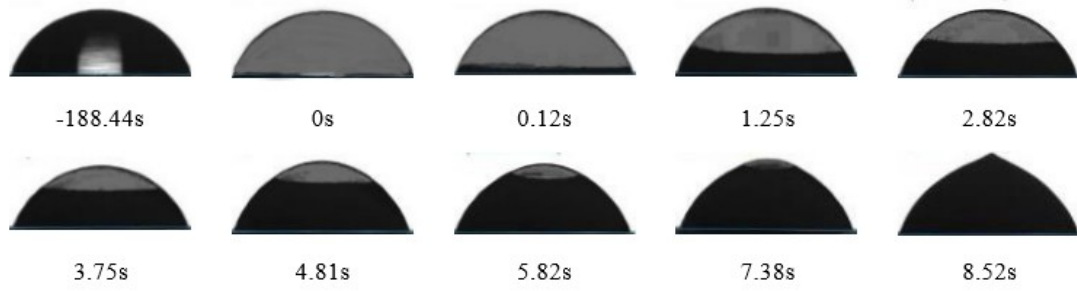
different substrate temperatures. The freezing process of droplets can be divided into two stages: supercooling stage and phase transition stage. The droplets were transparent in the supercooled stage and were entirely liquid in this stage. The lower the substrate temperature, the shorter the supercooling time, as expected. As shown in Fig. 5 (c), when the substrate temperature was -13.5°C, supercooling was completed in 188.44 s for droplet. In Figure 5 (a), when the substrate temperature was -7.5°C, the supercooling time was 808.69 s, about 4-fold increase. In the supercooling stage, the droplets were cooled sufficiently so that they reached the saturated liquid state and began to change phase. The inner part of the droplet near the metal surface was transformed to a solid-liquid mixture, and its transparency was accordingly reduced. Within about 3 s, the droplet phase transformation speed was faster and the solid phase height increased rapidly to half of the droplet height. After about 3 s, the advancing rate of the solid-liquid interface slowed down. As shown in Figures 5 (a) (b) (c), the solid-liquid interface reached half of the drop height at 3.66 s, 2.96 s and 2.82 s respectively, and reached the top of the drop at 11.82s, 9.99s and 8.52s respectively. This slowing down of the interface propagation was because the increase of the solid phase height increased the thermal resistance between the remaining liquid phase and the cold surface, due to which the heat transfer rate slowed down. In addition, the contact area of the solid-liquid interface was also reduced, as seen in figure 5, and so the heat transfer area was reduced. At the completion of the phase transformation, the droplets formed a bulge similar to the tip of a peach.
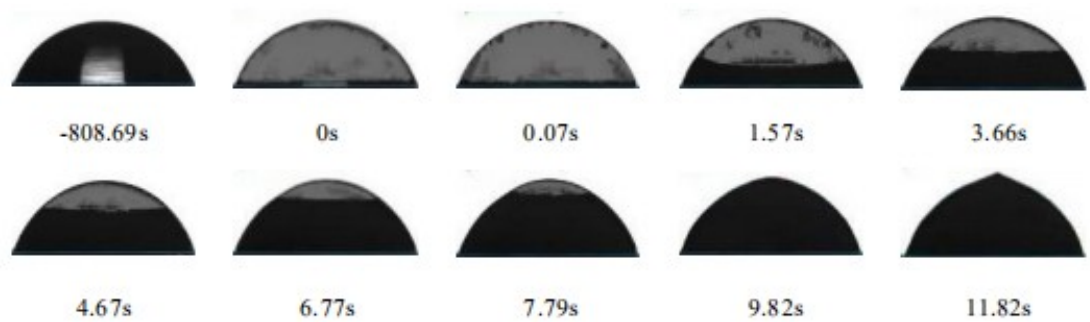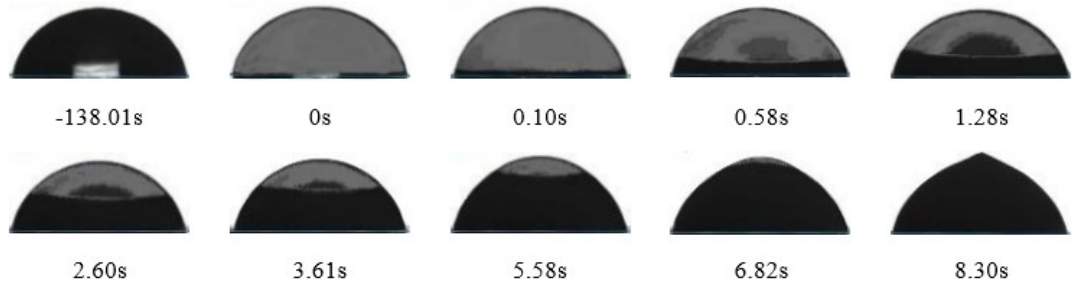

(a) Tw=-7.5°C.

(b) Tw=-10.5°C.

(c) Tw=-13.5°C.

(d) Tw=-17.5°C.

FIGURE 5 Freezing process of droplets under different substrate temperatures (φ=62%, V=5μL).

From Figures 5 (c) and (d), we compared the time of each stage of droplet freezing at -13.5°C and -17.5°C

and concluded that the difference between them was very small. The supercooling time was less than 200 s, and

the total freezing time was less than 9 s in both cases. The above comparison showed that in these two cases, the

droplet began to phase change before the substrate temperature dropped to the stable value. To better understand

the freezing process, the times for the various cooling/freezing phases have been plotted as a function of the

substrate temperature in Figure 6 (a). It can be seen from the figure that the supercooling time decreases with a

decrease in the substrate temperature. Moreover, the rate at which the supercooling time decreases also drops as

the substrate temperature decreases. This is due to increased transfer as a result of increased temperature difference

between the droplet and the substrate as the substrate temperature is reduced. It can be seen from Fig. 6 (a) that the

phase transition time of droplet is very short. In order to observe the change of phase transition time more

intuitively, it is separately plotted in Fig. 6 (b). It can be seen from the figure that the changing trend of phase

transition time is similar to that of supercooling time.
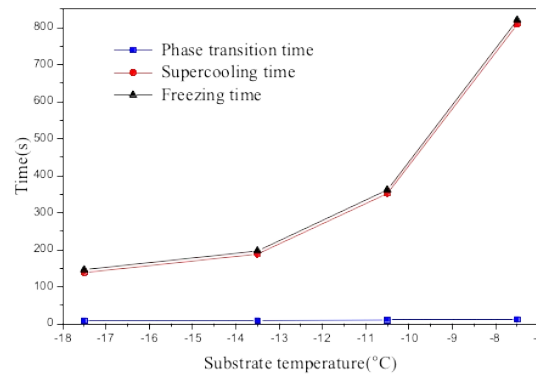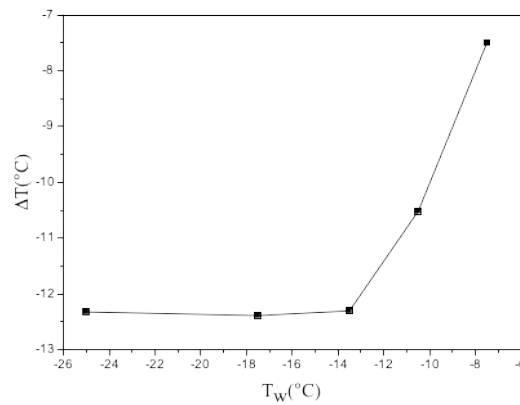

(a) Freezing time
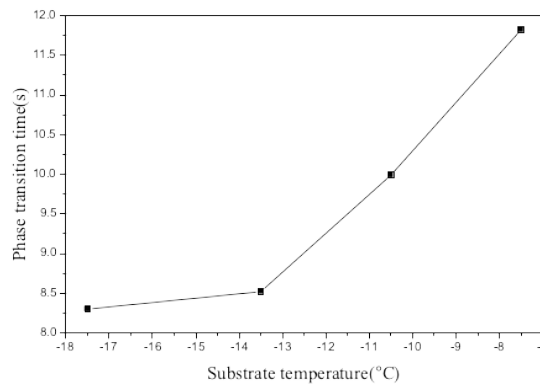
(b) Phase transition time

FIGURE 6 Freezing time under different substrate temperatures (φ=62%, V=5μL).

Figure 7 shows the change of the supercooling degree (ΔT) required for phase transformation to be initiated

in the droplet at different substrate temperatures. The supercooling degree of droplet is the difference between the

actual crystallization temperature and the theoretical crystallization temperature. At standard atmospheric pressure,

the theoretical crystallization temperature of the droplet is 0 °C. The supercooling degree of the droplets had an

obvious decreasing trend with a decrease in the substrate temperature. When the cold surface temperature was less

than - 13.5 °C, the supercooling degree required for droplet phase transformation to begin tended to a constant

value, i.e., a critical supercooling degree was found to exist. It can be seen from the curve in Fig. 7 that the critical

value of supercooling was about -12.3°C. Combined with Figure 6, it is seen that before reaching the critical

supercooling degree, the supercooling time decreased sharply with a decrease in the substrate temperature. The

phase transition time also decreased. When the critical supercooling degree was reached, the decreasing rate of

supercooling time and phase transition time of the droplets diminished, and the values tended to remain unchanged

thereafter. This was because when the substrate was relatively colder, the temperatures of the droplets could reach

the required supercooling quickly, which completed the nucleation and phase transformation in a very short time.

The above results show that the effect of the substrate temperature on the freezing time of droplets is closely

related to the critical supercooling degree. Increased critical supercooling value would decrease the driving force

for droplet phase transformation, thus prolonging the supercooling time of droplet, and vice versa.

FIGURE 7 Supercooling under different substrate temperatures (φ=62%, V=5μL).
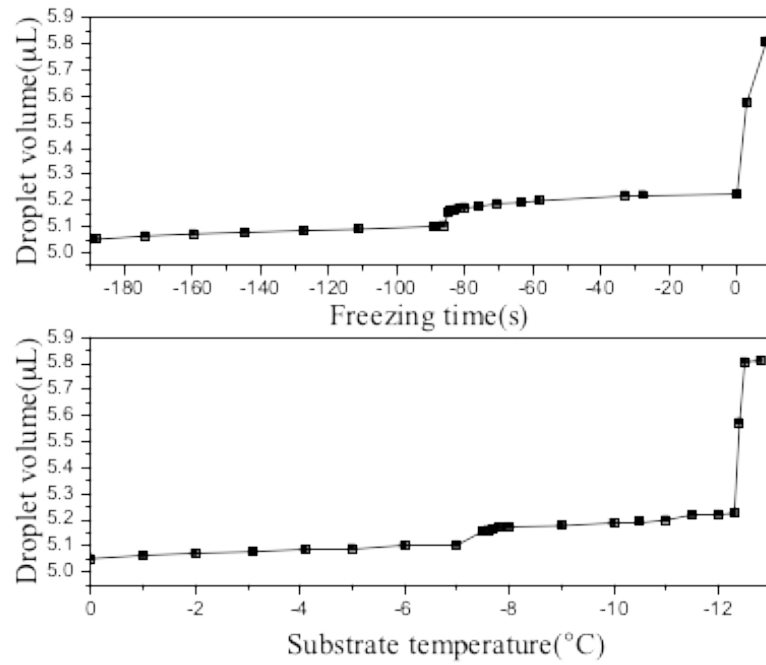
3.1.2 | Droplet shape

Fig. 8 shows how the solid-liquid interface profile evolves in the process of droplet (5μL) freezing. The substrate temperature was -13.5°C. It can be seen from the figure that the phase transformation of the droplet involved the solid-liquid interface advancing through the liquid region. In the process of the phase transition, the solid-liquid interface was consistently concave, moving upward from the bottom of the droplet. The transparency of the droplets gradually decreased as freezing progressed. According to the crystal growth theory, the solid-liquid interface tension will generate additional pressure perpendicular to the interface, reduce the interface area, and cause the solid-liquid interface to propagate upward. In this process, the change of density caused an increase of droplet volume, which resulted in the unfrozen liquid region being pushed upward. The implication of the solid-liquid interface being concave, is that the the droplet boundary froze more rapidly compared to the interior. Finally, when the phase transformation of the droplet was completed, the liquid film at the top broke, resulting in a pointed bulge. The formation of the bulge marked the end of the phase transformation.
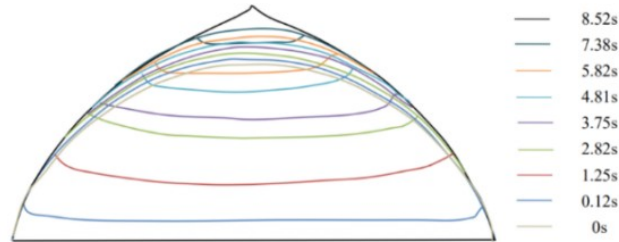
FIGURE 8 Evolution of the droplet profile and solid-liquid interface in the freezing process (Tw=-13.5°C, φ =62%, V=5μL).

Figure 9 shows the volume change of the droplet during freezing. Before -83.44s, the water vapor in the air condensed and the volume of the droplets increased gradually, from the original titration volume of 5.051μL to 5.104μL. The surface area of the droplet in contact with air increased with the increase in the volume. At - 83.44s, due to the increase of droplet volume, the small droplets condensed nearby were swallowed up, and the droplet volume changed suddenly. From -83.44s to 0s, with a decrease in the substrate temperature, the amount of water

vapor condensation in the air increased. The volume further increased from 5.104μL to 5.22μL. Thus, in about the

same time, the volume change was about 2 times that of the original. At 0 s, the droplet temperature reached

critical supercooling, and the phase transformation was subsequently completed in 8.52 s. In the phase

transformation stage, the volume growth was 0.581μL. The above results show that the volume change caused by

the condensation of water vapor in the air was very small, and the increase in volume was mainly due to the

density change as a result of the droplet freezing. When the freezing was completed, the volume of the droplet

increased to 1.16 times of the original, which was within a reasonable range of the expected change.

FIGURE 9 Change of droplet volume (Tw=-13.5°C, φ=62%, V=5μL).

According to the change process of droplet shape in Fig. 8, once the droplet begins to freeze, the bottom

shape will be fixed, and the deformation only occurs in the upper unfrozen part, and the contact angle will not

change. But in the supercooling stage, the contact angle will change with the change of volume. Therefore, this

experiment only studies the change of contact angle during the supercooling stage. Fig. 10 shows the change of

contact angle during supercooling, which is recorded when the temperature drops to 0 °C. In the supercooling

stage, the contact angle increases gradually. This indicates that the contact angle increases with the increase of

15
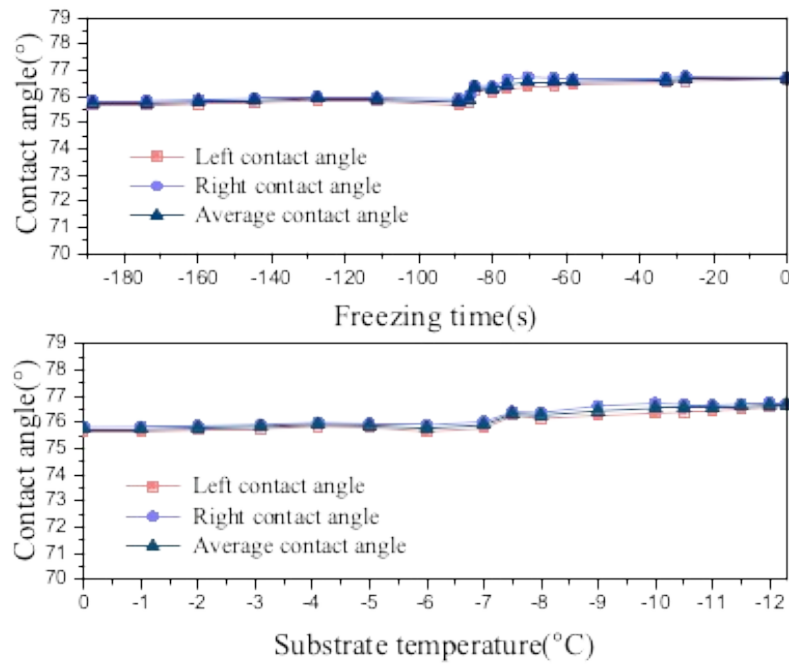
volume.

FIGURE 10 Change of contact angle during the supercooling stage (Tw=-13.5°C, φ=62%, V=5μL).
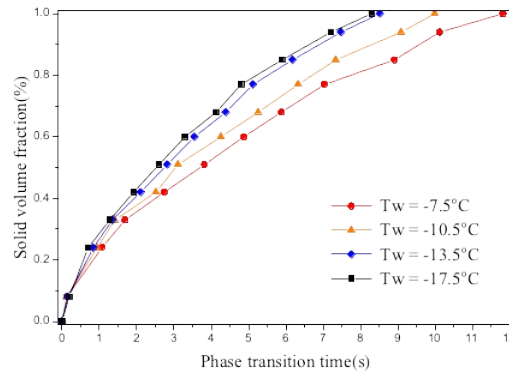
3.1.3 | Solid volume fraction

As seen from section 3.1, the phase transformation of droplets involves the solid-liquid interface advancing

through the liquid phase. In order to better understand the propagation of the solid-liquid interface in the droplet

freezing process, the time rate of change of the solid volume fraction (γ) was examined. γ is the ratio of the height

of the solid phase to the final height of the droplet. The final height of the droplet is its height after the droplet

completely freezes and forms a bulge. γ=0 thus represents the liquid phase, γ=1 represents the solid phase and γ

between 0 and 1 represents a solid-liquid mixture.

Fig. 11 shows how the solid volume fraction of the droplet changes with time at different substrate

temperatures. At the beginning of the phase transformation, the growth rate of the solid-phase height for the first

approximately 0.3 s was relatively fast. This was because, at the beginning of the phase transformation, the

temperature of the droplet was low enough to meet the supercooling requirements, and it could freeze very quickly.

With the occurrence of phase transformation, the solid-liquid interface moved upward. The heat transfer resistance between the metal surface and the liquid increased as the solid phase grew. At the same time, the contact area between the liquid and the solid decreased, and the heat transfer rate therefore slowed down due to both these effects, which resulted in any further increase in the solid volume requiring more time. After 0.3s, the solid volume fraction increased at a uniform rate. The lower the substrate temperature, the faster the phase interface moved upward. This was because the thermal conductivity (λ) of the ice was inversely proportional to its temperature (Eq.(1))[32]. The lower the temperature, the greater the thermal conductivity. When the substrate temperature was lower than the critical supercooling value (-13.5°C, -17.5°C), the droplets started to freeze even before the substrate temperature reached the set value. Therefore, the substrate temperature had little effect on the phase transformation process of the droplets, and the phase transformation time tended to be stable.

$$\lambda = \frac{488.19}{T} + 0.4685 \tag{1}$$

FIGURE 11 Change of solid volume fraction at different substrate temperatures (φ=62%, V=5μL).

The following normalized model was developed to predict the solid volume fraction as a function of the dimensionless temperature difference and the dimensionless time:

$$\gamma = 0.71531 \left(\frac{T_{air} - T_w}{T_{air}} Fo \right)^{0.58975} \tag{2}$$

17

In equation (2), $Fo = \dfrac{\alpha t}{R^2}$ represents the Fourier number (dimensionless time) which in turn depends upon

the initial thermal diffusivity $\alpha \left(\dfrac{k}{\rho c_p} \right)$ of the water droplet and the initial radius R $\left(\sqrt[3]{\left(\dfrac{3V}{4\pi} \right)} \right)$ of a spherical

droplet having the volume V. k is the thermal conductivity, ρ is the density, and c_p is the specific heat of the water

droplet, all properties to be calculated at the initial droplet temperature and pressure. Equation (2) can predict
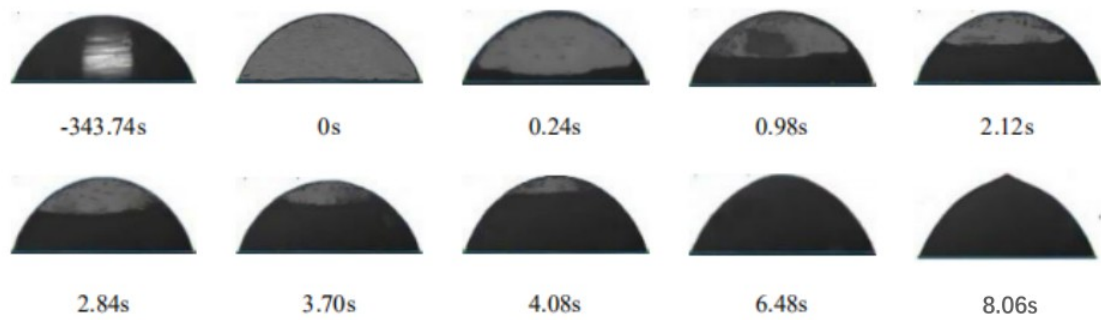
97.9% of the data in Figure 11 within ±10%.

From the above discussion, it can be concluded that the effect of the substrate temperature on the freezing

process of droplets is related to the degree of supercooling. Before the temperature reaches supercooling, the

droplets are in the supercooling stage. Once the temperature reaches the supercooling required by the droplet phase

transformation, the droplet nucleation occurs immediately. The lower the substrate temperature, the shorter the

supercooling time and phase transformation time. When the substrate temperature is lower than the critical

supercooling degree, the temperature of the droplet rapidly reduces to the value of the supercooling degree

required for phase transformation, and the supercooling time shortens. Therefore, conditions tending to increase

the critical supercooling temperature will also prolong the supercooling time of the droplets. In addition, the

volume of the droplets increases during the freezing process, which is mainly due to the decrease of the density

during the phase transformation.

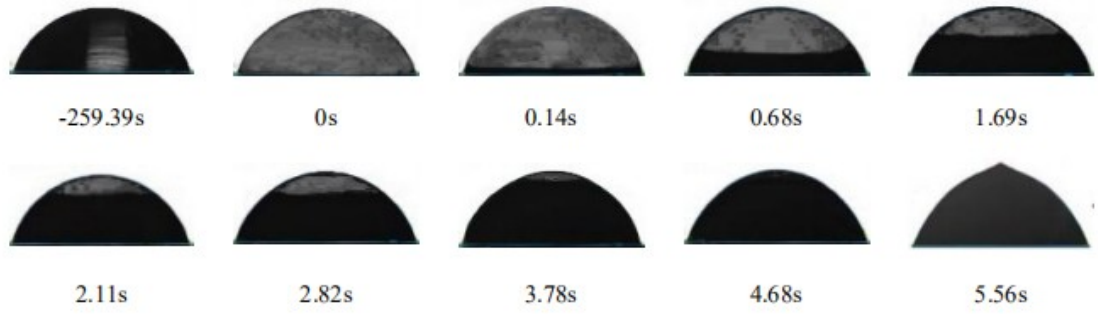## 3.2 | The effect of ambient relative humidity

3.2.1 | Freezing process

Figure 12 shows the freezing process of 5 µL droplets at different substrate temperatures when the ambient

relative humidity was maintained at 32%. The supercooling time was seen to decreased with a decrease in the

substrate temperature. This trend was similar to that depicted in Fig. 5. Compared to Fig. 5, at identical substrate
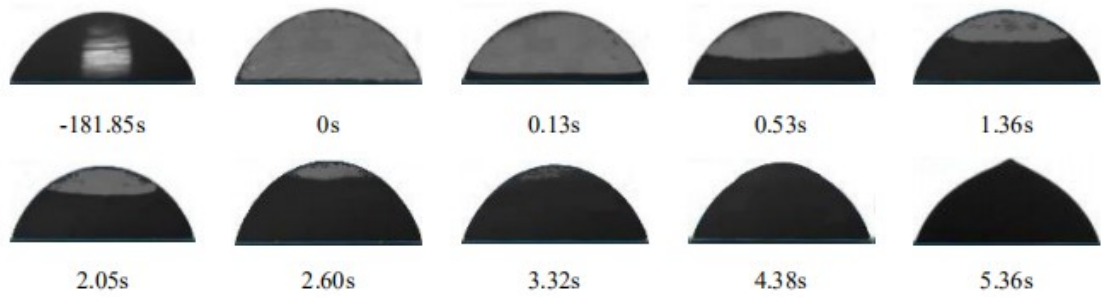
temperature, the supercooling time and the phase transformation time of the droplets were shortened with a decrease in relative humidity. In Figure 12 (a), the supercooling time and phase transformation time of droplets were 343.74s and 8.06 s. In Fig. 5 (a), the corresponding times were 808.69s and 11.82s, which were 2.35 times and 1.37 times those in Figure 12(a) respectively. When the substrate temperature approached the critical supercooling value, the effect of relative humidity on the droplet supercooling process was seen to weaken. As shown in Figure 12 (c), the supercooling time of the droplet was 181.85 s, and in Figure 5 (c), it was 188.44 s. However, under the same conditions, relative humidity did influence the phase transformation process. At identical substrate temperature, even if it was lower than the critical supercooling degree, the phase transformation time was seen to shorten with a decrease in the relative humidity. In Fig. 5 (c), the time for the solid phase to reach half the droplet height was 2.82 s, and the phase transition time was 8.52 s. In Figure 12 (c), these times were 1 s and 5.36 s, respectively. The above results show that the influence of relative humidity on the supercooling process is closely related to the critical degree of supercooling. When the supercooling degree reaches the critical value, the relative humidity has negligible effect on the supercooling time.
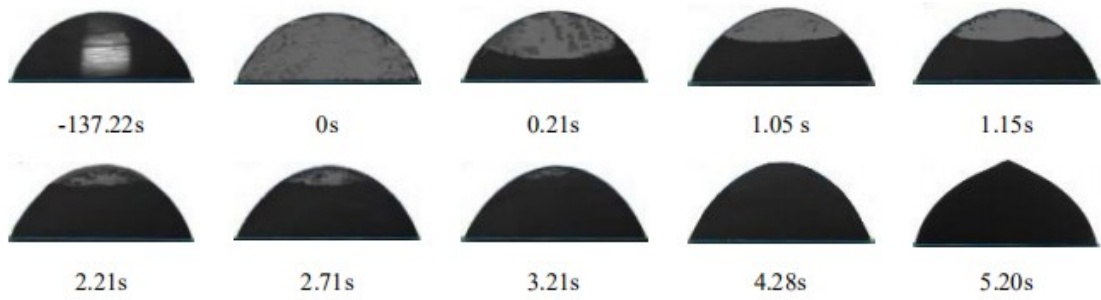

| -343.74s | 0s | 0.24s | 0.98s | 2.12s |
| 2.84s | 3.70s | 4.08s | 6.48s | 8.06s |

(a) Tw=-7.5°C.

| -259.39s | 0s | 0.14s | 0.68s | 1.69s |

| 2.11s | 2.82s | 3.78s | 4.68s | 5.56s |

(b) Tw=-10.5°C.

| -181.85s | 0s | 0.13s | 0.53s | 1.36s |

| 2.05s | 2.60s | 3.32s | 4.38s | 5.36s |

(c) Tw=-13.5°C.

| -137.22s | 0s | 0.21s | 1.05 s | 1.15s |

| 2.21s | 2.71s | 3.21s | 4.28s | 5.20s |

(d) Tw=-17.5°C.

FIGURE 12 Freezing process of droplets at different substrate temperatures (φ=32%, V=5μL).

To better explore the influence of the substrate temperature and the ambient relative humidity on the freezing time, Figure 13 compares the freezing time of the droplets under different working conditions. Fig. 13 (a) shows the change in the supercooling time. The higher the relative humidity, the faster the moisture in the air condensed into the droplet, which resulted in an increased thermal load on the cold plate. Therefore, at the same plate temperature, the supercooling time increased with an increase in the relative humidity. However, with a decrease in

the substrate temperature, the difference in supercooling time under different humidity conditions was seen to decrease. When the substrate temperature is lower than - 13.5 °C, the supercooling time is almost the same under different relative humidity conditions. This indicates that the influence of the relative humidity on the supercooling time decreased with a drop in the substrate temperature. When the substrate temperature was lower than the critical supercooling degree, the relative humidity had no effect on the supercooling time. Fig. 13 (b) presents the change in the phase transition time as a function of the substrate temperature for different values of the relative humidity. The trend for the phase transformation time with changing substrate temperature was similar under different relative humidity conditions. The lower the plate temperature, the shorter the phase transformation time was, as expected. Moreover, the rate of decrease in the phase transformation time dropped with a decrease in the substrate temperature. At the same substrate temperature, the phase transformation time decreased with a decrease in the relative humidity, which is related to the increased latent heat released by the increased rate of condensation of water vapor in the air, as discussed above. These results show that the change in phase transformation time can be positively correlated with the substrate temperature as well as the ambient relative humidity. The lower the plate temperature and ambient relative humidity, the shorter the phase transformation time.
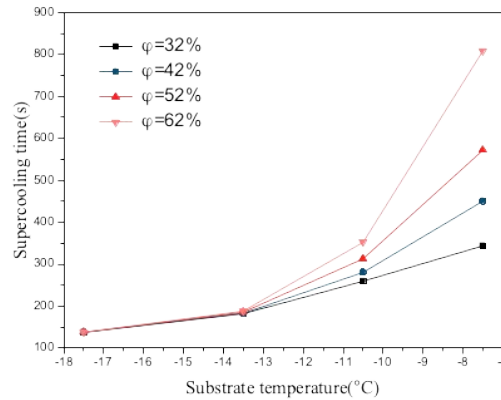
(a) Supercooling time.
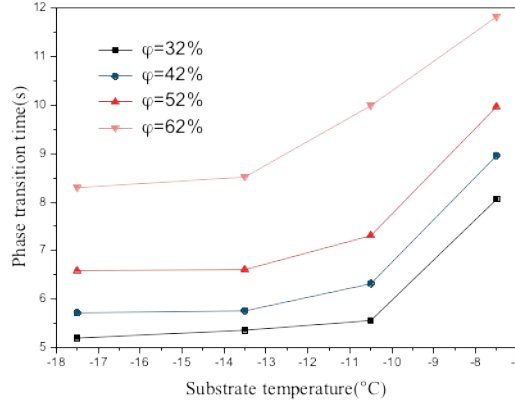
(b) Phase transition time

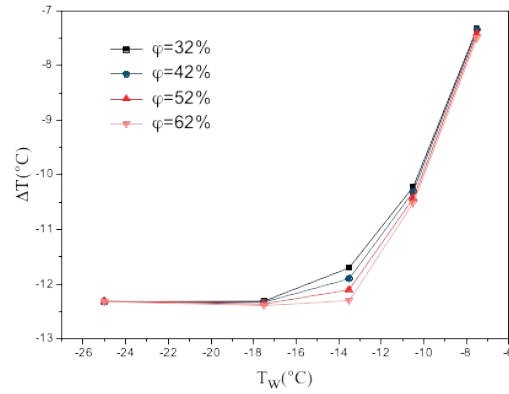**FIGURE 13** Freezing time under different working conditions (V=5μL).

The following normalized model was developed to predict the dimensionless supercooling time as a function

of the dimensionless temperature difference and the dimensionless humidity ratio difference:

$$Fo = \left(0.007497 + 0.114112\left(\frac{T_{air} - T_w}{T_{air}}\right)\ln\left(\frac{T_{air} - T_w}{T_{air}}\right) - 0.0524\left(\frac{\omega_{air} - \omega_w}{\omega_{air}}\right)^3\right)^{-1} \quad (3)$$

In equation (3), $Fo = \dfrac{\alpha t}{R^2}$ represents the Fourier number (dimensionless time) as in equation (2), which in

turn depends upon the initial thermal diffusivity α of the water droplet and its initial radius R. ω is the humidity

ratio of the air; ω_{air} is to be calculated at the temperature and pressure of the air surrounding the droplet, while

ω_w is calculated at the same air pressure and the temperature of the substrate under saturated conditions. Equation

(3) can predict 75% of the data in Figure 13 (a) within ±10% and 93.8% of the data within ±12%.

Fig. 14 shows the change in the supercooling degree (ΔT） at which the frost nucleation was initiated in the

droplet under different ambient relative humidity (φ) conditions. As can be seen from the figure, with an increase

in ambient relative humidity, the growth rate of supercooling increased. This was because the higher the relative

humidity of the air, the easier it became for the water vapor in the air to condense. This increased rate of

condensation of water vapor into the droplet released more latent heat, and more energy was thus needed to make

the droplet change its phase. However, the critical supercooling value did not change with the change of relative

humidity. These results suggest that the ΔT of the droplets could be increased by decreasing φ and increasing Tw

before the ΔT reached the critical value.

FIGURE 14 Supercooling degree under different working conditions (V=5μL).

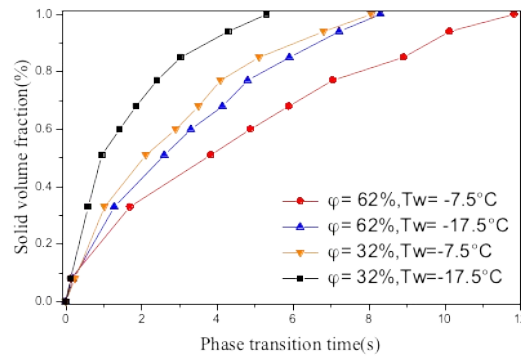## 3.2.2 | Solid volume fraction

Figure 15 shows the change in the solid volume fraction of the droplets as a function of time when the

ambient relative humidity was 32%. It can be seen from the figure that at the beginning of phase transformation,

the solid volume growth rate was faster as explained in connection with Figure 11. As time progressed, the height

of the solid phase increased, and the growth rate slowed down. The higher the substrate temperature, the slower the

growth rate of the solid volume fraction, as expected.
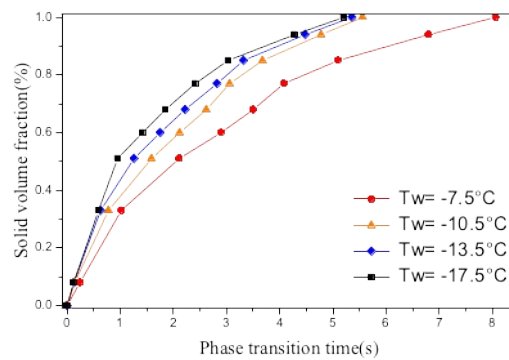
FIGURE 15 Change of solid volume fraction under different substrate temperatures (φ=32%, V=5μL).

To compare the effect of the ambient relative humidity and the substrate temperature on the droplet phase

23

transformation process, the change in the solid volume fraction under different conditions was plotted, as shown in

Figure 16. The growth rate of the solid volume fraction presented trends similar to those discussed above, i.e., the

growth was faster in the early stages and slowed down as time passed. At the same ambient relative humidity, the

lower the substrate temperature, the faster the solid volume fraction growth rate was. When the substrate

temperature was -7.5°C and the ambient humidity was 32%, the solid volume fraction reached 0.5 in 2s, and 1 in

8.06s. When the substrate temperature was reduced to -17.5°C, the solid volume fraction reached 0.5 in 1s, and 1

in 5.3s. The time required was about half or more than that at -7.5°C. At the same temperature, the smaller the

relative humidity, the faster the solid volume fraction increased. When the temperature of the substrate was -

17.5°C and the humidity was 62%, it took 2.6s for half-height solidification and 8.3s for complete solidification.

The necessary time was double that at 32% relative humidity. These results show that the substrate temperature

and the ambient relative humidity strongly affect the phase transformation rate of droplets. The lower the relative

humidity and the lower the substrate temperature, the faster the phase transformation rate will be, as expected.

FIGURE 16 Change of solid volume fraction at different conditions (V=5μL).

From the above discussions, it can be concluded that the influence of the ambient relative humidity and the

substrate temperature on the supercooling time are related to the degree of supercooling. When the supercooling

degree is higher than the critical value, the supercooling time can be prolonged by decreasing the relative humidity

or increasing the substrate temperature. When the supercooling degree reaches the critical value, the ambient
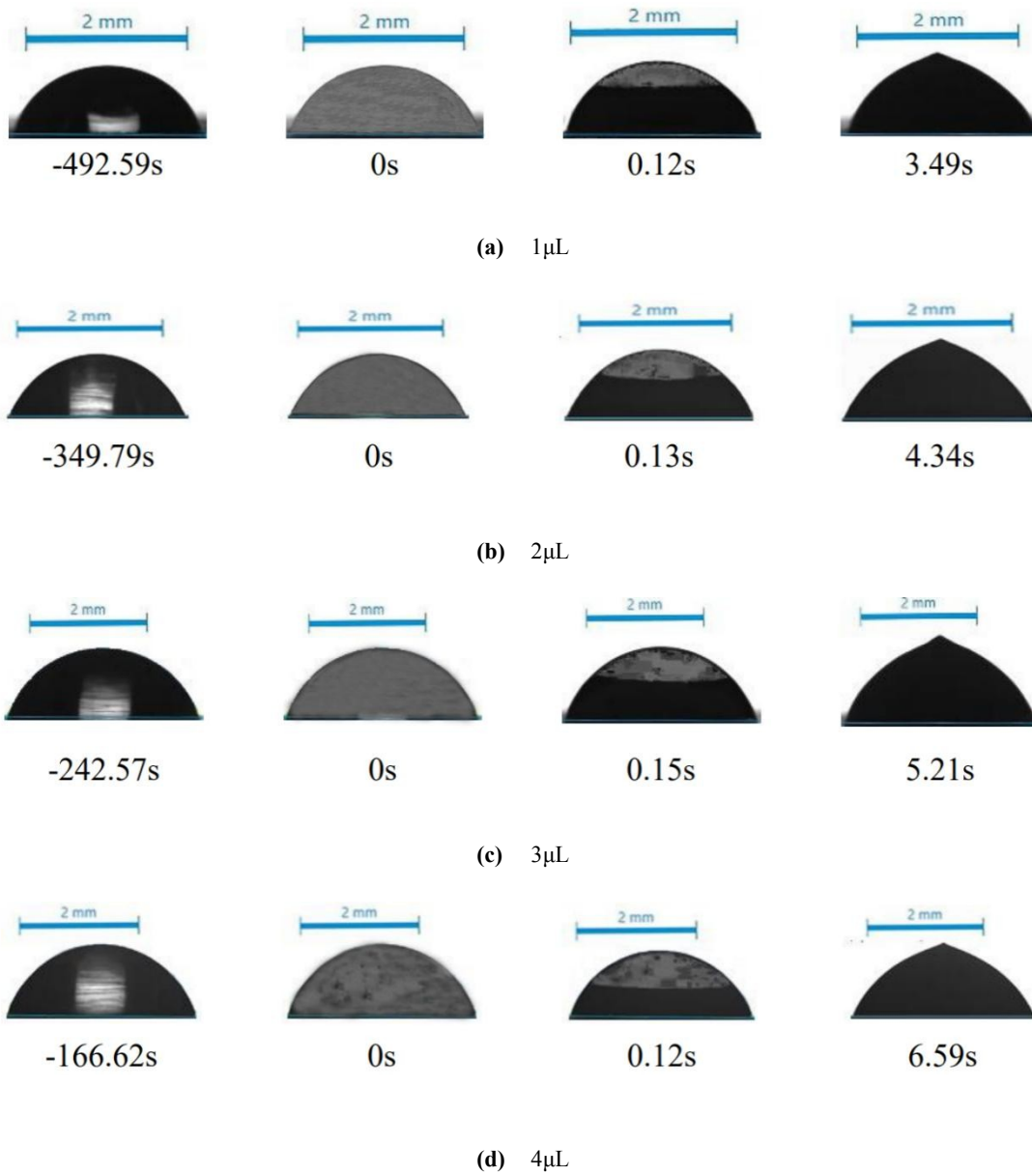
relative humidity has no effect on the supercooling time. The effect of substrate temperature on supercooling time will also be significantly weakened. So, the supercooling time can be prolonged by increasing the critical supercooling degree. In addition, the phase transformation time and the transformation rate are independent on the supercooling degree. They depend on the temperature of the substrate and the relative humidity of the environment. The lower the temperature of the substrate and the lower the relative humidity of the environment, the shorter the phase transformation time and thus, the faster will be the phase transformation rate.
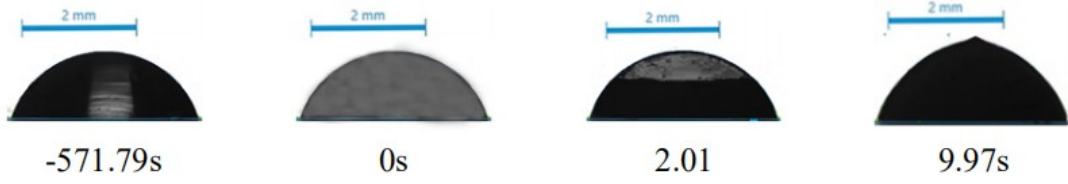
3.3 | The effect of droplet volume
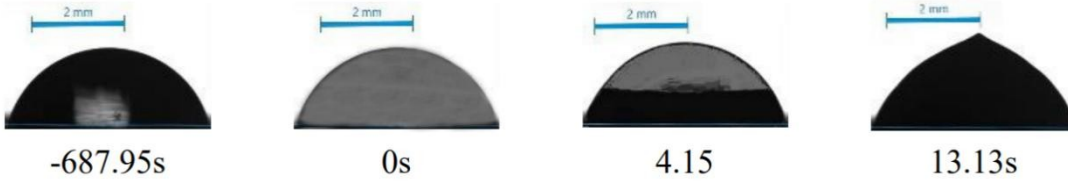
3.3.1 | Freezing process

In the process of droplet freezing, the intermolecular forces between the water molecules need to be strengthened in order to change phase. So, for different droplet volumes, the energy required to be rejected to strengthen the intermolecular forces is different, and hence, the freezing time is also different. Fig. 17 is an image sequence of the freezing process of different volume droplets (1 μL ~ 10 μL). The substrate temperature was -7.5°C, and the ambient relative humidity was 52%. From Figure 18, we can see that there was a significant positive correlation between the phase transition time and the droplet volume. This was attributed to the increased droplet volume (hence, mass) requiring more energy to strengthen the intermolecular forces. However, the change in supercooling time with droplet volume was non-monotonic. It can be seen from Figure 17 (a),(b),(c),(d) that when the droplet volume was less than 4 μL, the supercooling time decreased with volume. The supercooling time was 492.59s at 1 μL and 166.62s at 4 μL, and was seen to reduce consistently. In Figure 17 (d),(e),(f),(g),(h), the volume was equal to or larger than 4 μL, and the supercooling time increased with increasing volume. When the volume was 10μL, the supercooling time was 862.67s, which was 5.2 times that at 4 μL. This trend can be explained based on two opposing factors, as follows: (a) the supercooling time is directly related to the rate of heat rejection from the droplet. With increasing droplet volume (hence, mass), the supercooling required for phase

transformation would increase, the supercooling time required for phase transformation to begin would therefore increase. (b) However, at the same time, the contact area between the droplet and the substrate is also increasing with the droplet volume, thereby increasing the heat transfer rate between the substrate and the droplet for larger droplets. This factor would tend to decrease the supercooling time. Up to 4 µL, factor (b) above predominates, while for droplet volumes exceeding 4 µL, factor (a) preponderates. Therefore, the change of supercooling time with droplet volume is non-monotonic, as seen in Figure 18.
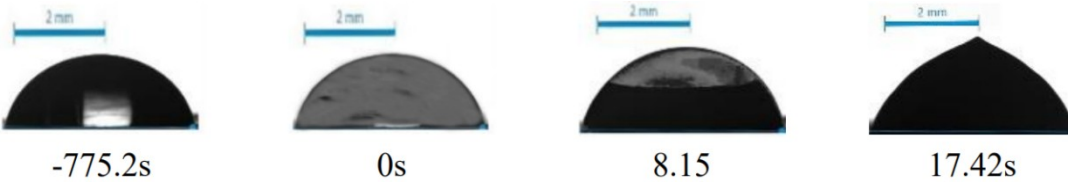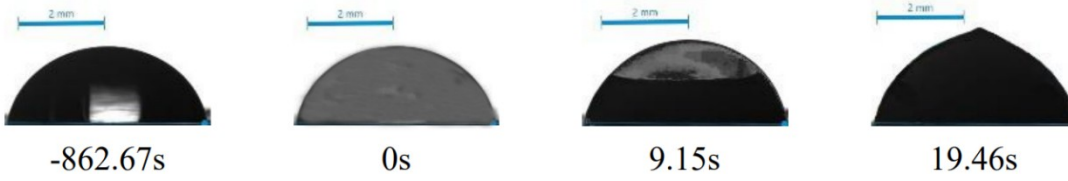

-492.59s   0s   0.12s   3.49s

(a)   1µL

-349.79s   0s   0.13s   4.34s

(b)   2µL

-242.57s   0s   0.15s   5.21s

(c)   3µL

-166.62s   0s   0.12s   6.59s

(d)   4µL

(e) 5μL

(f) 6μL

(g) 8μL

**(h)** 10μL

FIGURE 17 Freezing process of different volume droplets (Tw=-7.5°C, φ=52%).

To better understand these observations, the supercooling time is plotted as a function of droplet volume in Figure 18. With increasing droplet volume, the supercooling time decreased first and then increased. This non-monotonicity was because the increase in volume has two effects. On the one hand, the drop supercooling needed more cooling capacity, which tended to increase the supercooling time. On the other hand, with the increase of the contact area between the larger droplets and the cold surface, the cooling capacity transfer per unit time increased, which would tend to shorten the supercooling time of the droplet. There was thus a competitive relationship

27

between these two aspects. When the droplet volume was less than 4 μL, the second aspect played a leading role

due to the smaller droplet volume. With the increase of the droplet volume, the supercooling time and freezing

time of droplets were shortened. When the droplet volume was larger than 4 μL, the first effect was dominant. The

supercooling time and freezing time therefore increased with the increase in volume. However, as the volume

continues to increase, the first effect diminished in strength and the growth rate of the supercooling time

correspondingly slowed down. As can be seen from Figure 18, when the volume increased from 4 μL to 5 μL, the

supercooling time increased rapidly. And then the growth rate slowed down when the volume was larger than 5μL.

Extrapolating the trend in the figure, when the volume is more than 10 μL, the two effects may be equivalent, and

the supercooling time would become nearly constant. Future studies on the change of supercooling time with

different volumes (>10 μL) are therefore recommended.
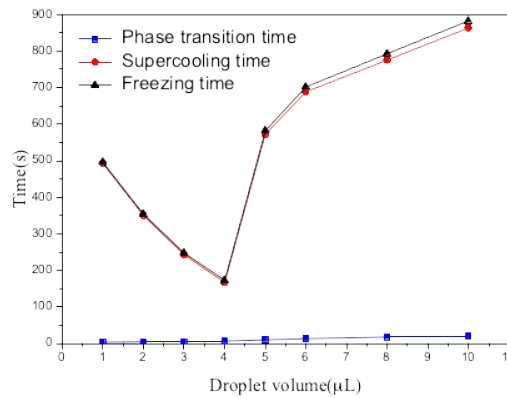
**FIGURE 18** Change of freezing time of different volume droplets (Tw=-7.5°C, φ=52%).

3.3.3 | Solid volume fraction change

Fig. 19 shows a comparison of the solid volume fraction changes for different droplet volumes. For a given

droplet volume, the growth rate of the solid volume fraction was rapid at the beginning of the phase transition, and

it then slowed down gradually. With an increase in droplet volume, the growth rate of the solid volume fraction

slowed down. For example, when the volume was 1μL, the droplet solidified to half its height in 1s and completely

in 3.49s. When the volume was 10μL, the corresponding times were 5s and 19.46s respectively. The solidification

time for the 10 μL droplet was thus 5.6 times that of the 1 μL droplet. This result can be attributed to two reasons.

One reason for this observation is that the droplet mass increased and the phase transition process needed to

strengthen greater number of intermolecular forces. Another reason is that the droplet height increased, the thermal

resistance to heat transfer between the substrate and the liquid phase increased. Due to both these effects, the heat

transfer rate slowed down, and the 10 μL droplet took longer to freeze.
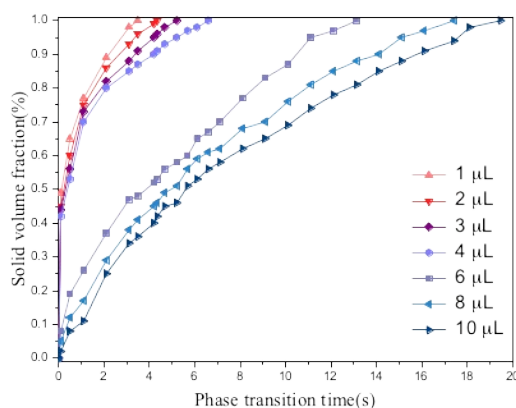
FIGURE 19 Change of solid volume fraction of different volume droplets (Tw=-7.5°C, φ=52%).

The following normalized model was developed to predict the solid volume fraction as a function of the

dimensionless time and the dimensionless droplet volume V*:

$$\gamma = 7.3226 + 1.1238\, lnFo + 1.2931 V^{\lambda} + 0.0465\left(lnFo\right)^2 - 1.08378\, V^{\lambda 2} + 0.05216\, V^{\lambda}\, lnF \quad (4)$$

It should be noted that equation (4) is valid for $Fo > 0$. In equation (4), $Fo = \dfrac{\alpha t}{R^2}$ represents the Fourier

number (dimensionless time) which in turn depends upon the initial thermal diffusivity α of the water droplet and

its initial radius R. $V^{\lambda} = \dfrac{V\left(\mu L\right)}{5}$ is a dimensionless droplet volume with reference to a 5 μL reference droplet

volume. Equation (4) can predict 75.7% of the data in Figure 19 within ±10% and 91.6% of the data within ±20%.

It can be seen from the above discussion that the change of supercooling time with volume is non-monotonic

because an increase in droplet volume results in two opposite effects. When the droplet volume is larger than or

smaller than the critical volume, the supercooling time trends in opposite directions. The supercooling time is the shortest when the volume of the droplet is 4 μL. However, the phase transition time of the droplet increases monotonously with the increase of the volume. The larger the volume, the slower the phase transformation rate , and the longer the phase transformation time.

4 | CONCLUSION

In this study, we experimentally investigated the effects of the substrate temperature, the ambient relative humidity, and the droplet volume on the freezing process of water droplets on a low-temperature copper plate. In the process of droplet freezing, there existed a critical degree of supercooling, which was about -12.3°C. The influence of the substrate temperature and the ambient humidity on the supercooling time were related to the critical degree of supercooling. Increasing critical supercooling could delay the freezing of droplets. The phase transformation time and transformation rate are found to be independent of supercooling. The phase transition time is positively correlated with substrate temperature and ambient relative humidity. The lower the substrate temperature and the relative humidity, the faster the phase transformation rate and the shorter the phase transition time. When freezing was completed, the volume of droplets would increase due to the condensation of water vapor in the air, and the change of the droplet phase from water to ice. The increase in the droplet volume in the phase transformation stage was significantly more than that in the supercooling stage.

The effect of droplet volume on the transformation time was monotonous. The larger the volume, the longer the phase transformation time was. However, the effect of volume on the supercooling time was not monotonous, and there was a critical droplet volume of 4 μL, below which the supercooling time decreased with increasing volume. When the droplet volume was larger than the critical value, it showed the opposite behavior.

At present, we have a clear understanding of the freezing process of droplets on a horizontal cold surface. This provides data and information which can be directly applied to the study of anti-icing cold surfaces. Further

research will be carried out to investigate the freezing process of droplets on cold surfaces with different inclined angles.

FUNDING INFORMATION

ACKNOWLEDGEMENTS

CONFLICT OF INTEREST

The authors declare no potential conflict of interest.

NOMENCLATURE

c_p specific heat of the water droplet, J/(kg·K)

k thermal conductivity of droplet, W/(m·K)

R droplet initial radius, $\sqrt[3]{\dfrac{3V}{4\pi}}$

Ra   surface roughness, nm

T temperature, °C

ΔT supercooling degree, °C

V droplet volume, μL

Greek Letters

α initial thermal diffusivity of the water droplet, $\dfrac{k}{\rho c_p}$

ρ density of water droplet, kg/m³

φ ambient relative humidity, %

λ thermal conductivity of ice, W/(m·K)

Non-Dimensional Numbers

γ solid volume fraction

ω humidity ratio of the air

Fo Fourier number, $\dfrac{\alpha t}{R^2}$

V^* dimensionless droplet volume, $\dfrac{V(\mu L)}{5}$

Subscripts

air   air

w   substrate

REFERENCES

1. Blake J D, Thompson D S, Tobias S. Simulating the freezing of supercooled water droplets impacting a cooled substrate[J]. *American Institute of Aeronautics and Astronautics*. 2014. https://doi.org/10.2514/6.2014-2328.

2. Israel B, Sebastiao B B, Serguei T, Satoshi O, Matthias P, Bernhard L, Alina A. Bulk dynamic spray freeze-drying part 1: Modeling of droplet cooling and phase change[J]. *Journal of Pharmaceutical Sciences*. 2019;108:2063-2074. https://doi.org/10.1016/j.xphs.2019.01.009.

3. Israel B, Sebastiao B B, Serguei T, Satoshi O, Matthias P, Bernhard L, Alina A. Bulk dynamic spray freeze-drying part 2: Model-based parametric study for spray-freezing process characterization[J]. *Journal of Pharmaceutical Sciences*. 2019;108:2075-2085. https://doi.org/10.1016/j.xphs.2019.01.011.

4. Wu X M, Hu S, Chu F Q. Experimental study of frost formation on cold surfaces with various fin layouts[J]. *Applied Thermal Engineering*. 2016;95:95-105. https://doi.org/10.1016/j.applthermaleng.2015.11.045.

5. Rahman M A, Jacobi A M. Experimental study on frosting/defrosting characteristics of microgrooved metal surfaces[J]. *International Journal of Refrigeration.* 2015;50:44-56. https://doi.org/10.1016/j.ijrefrig.2014.11.002.

6. Marín A G, Enriquez O R, Brunet P, Colinet P, Snoeijer J H. Universality of tip singularity formation in freezing water drops[J]. *Physical Review Letters.* 2014;113:054301. https://doi.org/10.1103/PhysRevLett.113.054301.

7. Oscar R E, Álvaro G M, Koen G W, Jacco H S. Freezing singularities in water drops[J]. *Physics of Fluids.* 2012;24:91102. https://doi.org/10.1063/1.4747185.

8. Md F I, Prashant R W. Universality in freezing of an asymmetric drop[J]. *Applied Physics Letters.* 2016;109:234105. https://doi.org/10.1063/1.4971995.

9. Schulte K, Weigand B. On the analytical modelling of the initial ice growth in a supercooled liquid droplet[J]. *International Journal of Heat and Mass Transfer.* 2018;127:1070-1081. https://doi.org/10.1016/j.ijheatmasstransfer.2018.06.089.

10. Zhang X, Liu X, Wu X M, Min J C. Simulation and experiment on supercooled sessile water droplet freezing with special attention to supercooling and volume expansion effects[J]. *International Journal of Heat and Mass Transfer.* 2018;127:975-985. https://doi.org/10.1016/j.ijheatmasstransfer.2018.07.021.

11. Zhang Xuan, Liu X, Min J C, Wu X M. Shape variation and unique tip formation of a sessile water droplet during freezing[J]. *Applied Thermal Engineering.* 2019;147:927-934. https://doi.org/10.1016/j.applthermaleng.2018.09.040.

12. Chaudhary G, Li R. Freezing of water droplets on solid surfaces: An experimental and numerical study[J]. *Experimental Thermal and Fluid Science.* 2014;57:86-93. https://doi.org/10.1016/j.expthermflusci.2014.04.007.

13. Zhang X, Wu X M, Min J C. Freezing and melting of a sessile water droplet on a horizontal cold plate[J].

Experimental Thermal and Fluid Science. 2017;88:1-7. https://doi.org/10.1016/j.expthermflusci.2017.05.00.

14. Vu T V, Dao K V, Pham B D. Numerical simulation of the freezing process of a water drop attached to a cold plate[J]. *Journal of Mechanical Science and Technology*. 2018;32:2119-2126. https://doi.org/10.1007/s12206-018-0421-4.

15. Haruka E, Shigeo K, Mitsugu H. Analysis of minute water droplet's freezing process on coated surface[J]. *SAE International*. 2013;6(2):2177. https://doi.org/10.4271/2013-01-2177.

16. Ludmila B , Alexandre M E, Vadim V K, Andrei S P. Effect of wettability on sessile drop freezing: When superhydrophobicity stimulates an extreme freezing delay[J]. *Langmuir*. 2014;30:1659-1668. https://doi.org/10.1021/la403796g.

17. Huang L Y, Liu Z L, Liu Y M, Gou Y J, Wang L. Effect of contact angle on water droplet freezing process on a cold flat surface[J]. *Experimental Thermal and Fluid Science*. 2012;40:74-80. https://doi.org/10.1016/j.expthermflusci.2012.02.002.

18. Yue X F, Liu W D, Wang Y. Freezing delay, frost accumulation and droplets condensation properties of micro- or hierarchically-structured silicon surfaces[J]. *International Journal of Heat and Mass Transfer*. 2018;126:442-451. https://doi.org/10.1016/j.ijheatmasstransfer.2018.04.165.

19. Hao P F, Lv C J, Zhang X W. Freezing of sessile water droplets on surfaces with various roughness and wettability[J]. *Applied Physics Letters.* 2014. 104. https://doi.org/10.1063/1.4873345.

20. Schrem M , Tropea C. Solidification of supercooled water in the vicinity of a solid wall[J]. *Physical Reviewe.* 2016;94:052804. https://doi.org/10.1103/PhysRevE.94.052804.

21. Alidad A, Fang G P. Understanding the anti-icing behavior of superhydrophobic surfaces[J]. *Surface Innovations*. 2014;2(S12):94-102. https://doi.org/10.1680/si.13.00046.

22. Kuok C, Blake N, Kwang J K, Anupam K. Theoretical consideration of contact angle hysteresis using surface-energy-minimization methods[J]. *International Journal of Heat and Mass Transfer.* 2016;102:154-161. https://doi.org/10.1016/j.ijheatmasstransfer.2016.06.014.

23. Gao P H, Zhang M, Du Y J, Cheng B, Zhang D H, Zhou G Q. The cooling and freezing law of droplets under the action of ultrasonic[J]. *Journal of Chemical Industry and Engineering*. 2017;68(11):4095-4104. https://doi.org/10.11949/j.issn.0438-1157.20170381.

24. Gabyshev D N, Fedorets A A, Aktaev N E, Otto K, Andreev S N. Acceleration of the condensational growth of water droplets in an external electric field[J]. *Journal of Aerosol Science*. 2019;135:103-112. https://doi.org/10.1016/j.jaerosci.2019.06.002.

25. Tavakoli F, Davis S H, Kavehpour H P. Freezing of supercooled water drops on cold solid substrates: initiation and mechanism[J]. *Journal of Coatings Technology & Research*. 2015;12:869-875. https://doi.org/10.1007/s11998-015-9693-0.

26. Jin Z Y, Zhao Y P, Sui D Y, Yang Z G. The Effects of Ambient pressure on the initiation of the freezing process for a water droplet on a cold surface[J]. *Journal of Heat Transfer*. 2016;138:084502. https://doi.org/10.1115/1.4033377.

27. Sultana K R, Rope K, Lam L S, Muzychka Y S. Phase change and droplet dynamics for a free falling water droplet[J]. *International Journal of Heat and Mass Transfer*. 2017;115:461-470. https://doi.org/10.1016/j.ijheatmasstransfer.2017.08.049.

28. Ding B, Wang H, Zhu X, Chen R, Liao Q. Water droplet impact on superhydrophobic surfaces with various inclinations and supercooling degrees[J]. *International Journal of Heat and Mass Transfer*. 2019;138:844-851. https://doi.org/10.1016/j.ijheatmasstransfer.2019.04.106.

29. Yao Y N，Li C，Zhang H, Yang R. Modelling the impact, spreading and freezing of a water droplet on horizontal and inclined superhydrophobic cooled surfaces[J]. *Applied Surface Science*. 2017;419:52-62. https://doi.org/10.1016/j.apsusc.2017.04.085.

30. Yao Y N，Li C, Tao Z X, Yang R, Zhang H. Experimental and numerical study on the impact and freezing process of a water droplet on a cold surface[J]. *Applied Thermal Engineering*. 2018;137:83-92.

https://doi.org/10.1016/j.applthermaleng.2018.03.057.

31. Chaudhary G, Li R. Freezing of water droplets on solid surfaces: an experimental and numercial study[J]. *Experimental Thermal and Fluid Science*. 2014;57:86-93. https://doi.org/10.1016/j.expthermflusci.2014.04.007.

32. Hobbs P V. Ice Physics[M]. Oxford University Press, USA. 2010.